Surrogate Model for Ship Resistance: a Sensitivity Analysis of Shape Deformation

Antonio Coppedè*, Stefano Gaggero*, Giuliano Vernengo* and Diego Villa*
*Dept. of Electric, Electronic, Telecommunication Engineering and Naval Architecture (DITEN), University of Genova, 16145, Italy
antoniocoppede@gmail.com, stefano.gaggero@unige.it, giuliano.vernengo@unige.it, diego.villa@unige.it

1 Introduction

Shape optimization and sensitivity can now be considered a standard to design efficient ships and new unconventional hull forms. There might be very different strategies to achieve such a process, depending on many circumstances, both operational (e.g. available time windows for computations) and methodological (e.g. available numerical methods). As in most of the engineering cases, the best trade-off between accuracy of the solution and the time required to achieve it is searched. When using medium-fidelity methods e.g. Boundary Element Methods (BEMs) for wave resistance and seakeeping, population based optimization algorithm can still be a viable way to achieve a design solution (see e.g. Vernengo et al., 2015 or Vernengo and Brizzolara, 2017). However, when the solution of the quantity of interest becomes more demanding, alternative methods of searching through the design space are needed. In this perspective, a surrogate model based approach for hull form sensitivity analysis is presented. The method relies on the features of a Kriging response surface (see for instance Forrester et al., 2008) to interpolate few computed solutions and to predict the same solution over the whole explored domain. The sensitivity analysis focuses on the effect of hull form variations with respect to calm water resistance at a given forward speed. The total ship resistance is computed by means of a high-fidelity viscous solver based on the *openFOAM* libraries (Jasak et al., 2007). The shape variations are achieved by a combined approach specifically developed to preserve the fairness of the hull surface based on *Subdivision Surface* and *Free Form Deformation* (FFD) (Coppedé et al., 2018).
The hydrodynamic solver has been preliminary validated by comparison against available experimental measurements on the KRISO Container Ship (KCS) hull. The variation of the Kriging response surface performance with respect to different sizes of the initial sampling have been studied and possible optimum hull shape have been detected and compared in terms of calm water resistance, wave patterns and pressure on the surface.

2 Framework

The three main tools on which the framework for calm water resistance surrogate model generation relies on are described in the following sections.

2.1 Hull shape generation and variation

According to the combined approach proposed by Coppedé et al., 2018, the hull surface has been first generated by using the *QuadTri* Subdivision Surface algorithm (Stam and Loop, 2003). Based on an initial control polygon, made of both triangular and quadratic elements, this algorithm provides a smooth surface by a recursive subdivision of the initial control polygon itself. The final surface mesh is represented by a unique watertight patch. As a first result, this surface can be easily linked to numerical solvers avoiding conversion that might cause further unwanted geometric deviations. However, for complex hull forms e.g. with bulbows bow and stern skeg, such a surface is typically generated by using a relatively large number of control points. Since variations are in principle obtained by changing the three cartesian coordinates of those control points, this usually results in too many free parameters to be managed in the context of an optimization/exploration problem. Similarly to what have been proposed by Peri and Campana, 2003, in order to overcome this issue, FFD transformations (see Sederberg and Parry, 1986) have been applied to the control points of the Subdivision Surface rather than directly on the hull surface. Such an approach ensures the limit surface of the hull to be recreated by the *QuadTri* algorithm after each shape variation, hence excluding possible discontinuities or excessive

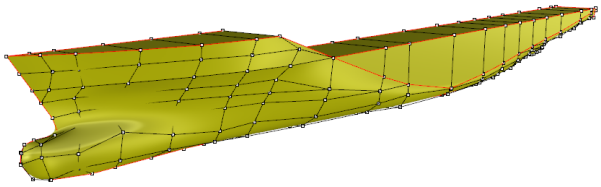

Fig. 1: KCS hull with Subdivsion Surface control polygon, where the red line describes the crease edges.

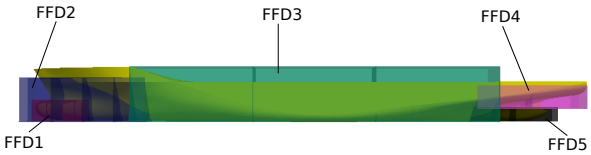

Fig. 2: Original Hull of the Kriso Container Ship (KCS) with five Free Form Deformation control volumes.

deformations of the patches. Moreover, by following this method the number of free parameters controlling the shape is drastically reduced, being the FFD transformations themselves the free variables of the optimization process.
The original KCS hull with its control polygon is represented in Figure 1 while the created FFD boxes are shown in Figure 2. This five boxes are designed to achieve both local and global shape variations. The FFD1 and FFD5 are designed for local variations of the bulbous bow and of the skeg, respectively. The FFD2 transformation acts on the bow hull shape while the FFD4 is defined over the upper stern rise. The FFD3 is instead used to modify a relatively long longitudinal part of the hull by moving afterward and forward the volume of the parallel body in a Lackemby's transformation fashion (Lackenby, 1950). In order to further simplify the deformation process the number of free parameters is reduced to seven by using analytic functions for FFD points variations. Hence, some selected control points of each FFD volume are modified at the same time according to the laws imposed by these mathematical functions.

2.2 High-fidelity CFD resistance computation

An open source viscous based RANS solver has been used to compute the calm water resistance of the ship. By using such a high-fidelity solver the influence on resistance of both global and local shape variations can be taken into account. The selected solver has already been proven to ensure reliable predictions of the KCS resistance (see among the other Gaggero et al., 2017, Villa et al., 2011 and Larsson et al., 2015). Results of the validation in terms of comparison between experimental and numerical total resistance coefficient C_T, sinkage and trim, respectively, are reported in Table 1. The hull surface and the domain have been discretized by using about 1.5 ML cells with specific refinements of the free surface close to the hull over a region where the wave field is supposed to propagate.
The comparison shows that the numerical prediction of the total resistance is in good agreement with the experimental measurements, especially in the range of higher speeds ($F_N > 0.2$) for which the relative error is less than 2%. At lower speeds ($F_N < 0.2$), the agreement is still very good but the error rise up to 5%. In all the tested cases such a relative error is lower than the experimental uncertainty, as shown in Figure 3. Running attitude of the ship are also well predicted as displayed in the comparison of the drafts at the aft and forward perpendicular, respectively.
Since each simulation run for about 30 hours on a 24 cores work-station a mesh coarsening analysis has been carried out in order to check the feasibility of using a lower number of elements, i.e. to reduce the computational burden while keeping a good accuracy of the solution. So other two coarsening levels have been considered, namely the Coarse L_1 mesh having 0.8 ML cells and the Coarse L_2 made of 0.4 ML cells. The CPU time required for the solution with the coarser mesh is five time lower compared to that needed with the finer mesh. Rather than an usual mesh sensitivity analysis based on the reference KCS hull, figure 4 displays the variation of the computed resistance obtained by using the three meshes

on 30 hull variations achieved by the combined approach above described. Since the design by optimization is focused on local shape variations it is crucial to verify the monotonicity of predictions at different discretization levels, being optimization designs based on reliable comparative analyses more than on absolute results. Each simulation has been performed at the same displacement, ensuring the static equilibrium condition (i.e. both longitudinal and vertical equilibrium) by proper rotation and translation of the hull. Except for two cases, the predicted values of the resistance are bounded within a small range of variation.

In addition the wave profiles at $y/L_{PP} = 0.2$ for the original hull computed by using the three meshes are shown in Figure 5. Throws and crests are predicted in the same location showing minor differences in terms of wave amplitude. This is a further confirmation that the coarser mesh can be used for the proposed sensitivity study since the analysis is mainly focused on the comparison of the solutions.

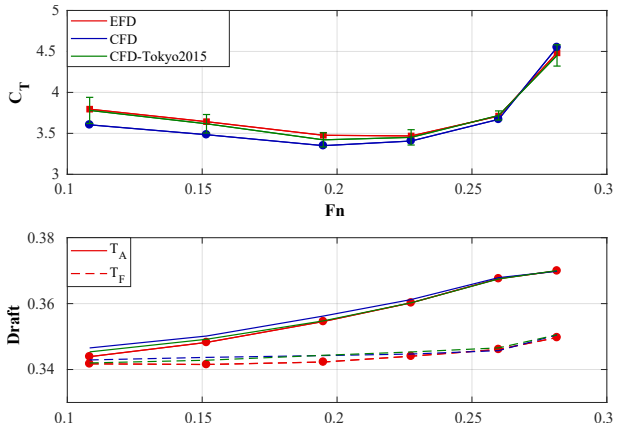

Fig. 3: Comparison of present CFD predictions (blue line) among EFD measurements (red line) and average CFD prediction reported in the Tokyo 2015 workshop (green line).

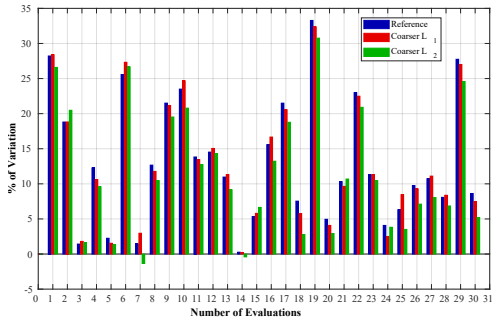

Fig. 4: Comparison of the hull drag trend (% of reference case) for 30 hull shape variations for reference (blue), Coarse L1 (red) and Coarse L2 (green) mesh densities.

Table 1: Comparison between experimental measurements (EFD) and numerical results (CFD) for the KCS test case

Model test		EFD			CFD		
Speed [m/s]	Fn	$C_T \cdot 10^3$	Sink [cm]	Trim [deg]	$C_T \cdot 10^3$	Sink [cm]	Trim [deg]
0.915	0.108	3.795	-0.089	-0.017	3.604	-0.274	-0.028
1.281	0.152	3.643	-0.273	-0.053	3.484	-0.478	-0.051
1.647	0.195	3.477	-0.599	-0.097	3.350	-0.781	-0.094
1.922	0.228	3.469	-0.950	-0.127	3.406	-1.031	-0.130
2.196	0.260	3.711	-1.394	-0.169	3.671	-1.386	-0.174
2.379	0.282	4.483	-1.698	-0.159	4.550	-1.736	-0.152

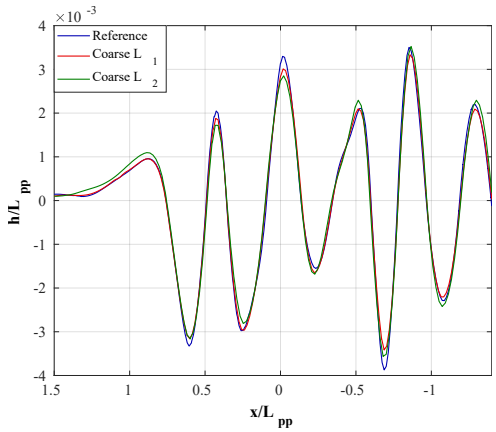

Fig. 5: Non-dimensional wave elevation for a longitudinal profile at y/L_{PP}=0.2.

3 Sensitivity analysis by Kriging response surface

The analysis of the size of the sampling on the performance of the Kriging response surface has been performed by using three sets of designs, made of 30, 60 and 120 geometries respectively. Two Cross-Validation methods have been applied to evaluate the prediction capabilities of the three surrogate models, namely the so-called *Leave-One-Out* (LOO) and the *k-fold* (see for instance Forrester et al., 2008). According to the *K-fold* model the DoE in divided into k subset. Each subset is then discarded from the generation of the surrogate model and the prediction error is evaluated by comparing the value obtained by the model with respect to the original value. This process is repeated for all the k subsets and the mean error of all k is finally computed. The LOO method can be considered as a particular case of a *k-fold* with $k = 1$, i.e. one design at the time is discard from the initial sampling. For both methods, the correlation coefficient and the Root Mean Squared Error (RMSE) are computed according to Eq. (1) and Eq. (2), respectively:

$$R^2 = \left(\frac{cov\left(\mathbf{r}, \widehat{\mathbf{r}}\right)}{\sqrt{var(\mathbf{r}) var(\widehat{\mathbf{r}})}} \right)^2 \tag{1}$$

$$RMSE = \sqrt{\frac{\sum_{i=1}^{n} \left(r_i - \widehat{r_i}\right)^2}{n}} \tag{2}$$

Results of this cross-validation are reported in Table 2. All the three surrogate models show good prediction capabilities having $R^2 > 0.8$ and $RMSE < 10\%$, respectively. As indicated by the increase of the R^2 and by the corresponding decrease of the $RMSE$, the accuracy of the Kriging model is increased for larger sampling.

The global *minima* of the three models have been searched by means of a classic genetic algorithm (GA) in order to avoid possible local optimal designs. Compared to the original KCS hull, the three designs achieve resistance reductions in the extent of 5.9%, 6.1% and 6.3% for the model with the lowest sampling size up to that with the larger one, respectively. Figure 6 displays the location of the three optimal designs on sub-spaces of the Kriging model based on the larger sampling (120 designs). Each sub-space is defined in the plane of two of the seven parameters at a time. The other five parameters are kept at

Table 2: Results of the LOO and *k-fold* cross validations of the three Kriging models.

Parameter	$KR_{\#30}$	$KR_{\#60}$	$KR_{\#120}$
R^2_{LOO}	0.947	0.948	0.973
$RMSE_{LOO}$	0.0887	0.0846	0.0462
R^2_{k-fold}	0.871	0.898	0.965
$RMSE_{k-fold}$	0.0838	0.0817	0.0542

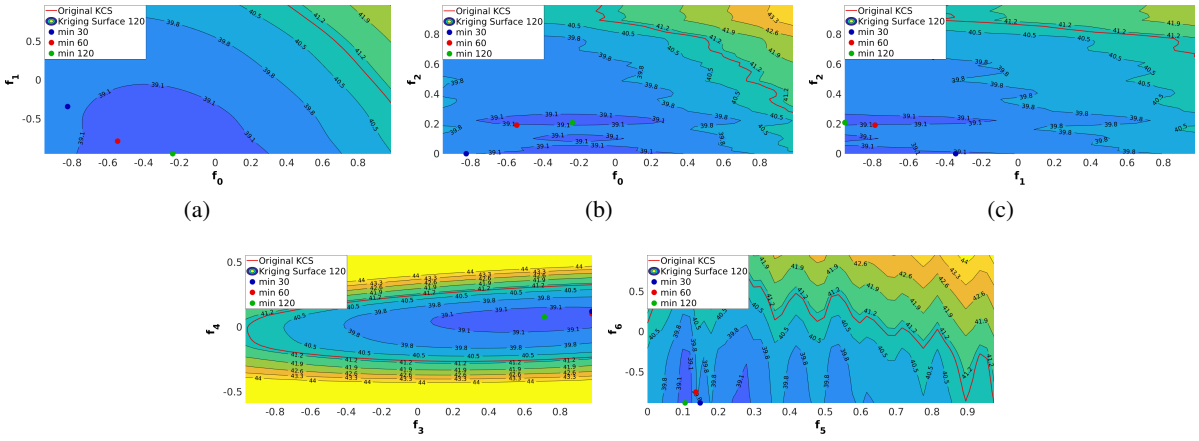

Fig. 6: Kriging surface generated with 120 design, the red contour of the original KCS and the projection of the three minimum obtained for all three model

the value corresponding to the optimum design of the Kriging with the largest sampling size. It is worth noting that the optimum designs for the first two surrogate models do not exactly lay on the presented planes, since they belong to different surfaces, hence to different combinations of the parameters. The three Kriging surrogate model provides different optimum designs since the three points are locate at different positions on each sub-space. The wave patterns of the three selected hull surfaces are compared to those of the original KCS hull in Figure 7 while Figure 8 displays the pressures over the three optimum hulls from the corresponding surrogate models. As expected both the wave patterns and the pressure distributions are very close one to the other. This is mainly due to the fact that neither the length at the design waterline of the ship or the length of the bulb have been significantly changed. Despite this, a common trend can be detected for all the three designed hulls. In particular, the wave pattern is slightly anticipated. The first divergent wave generated by the bulb of the optimized shape (red contours) propagates away from the hull with a higher local crest. It decays faster moving backwards towards the hull forward shoulder. In turn, also the divergent waves created at the forward shoulder is anticipated. This phase lag is kept in the far field wave pattern too. The optimized hulls produces lower waves aft of the transom stern. Those little variations are partially seen also on the dynamic pressures on the hulls.

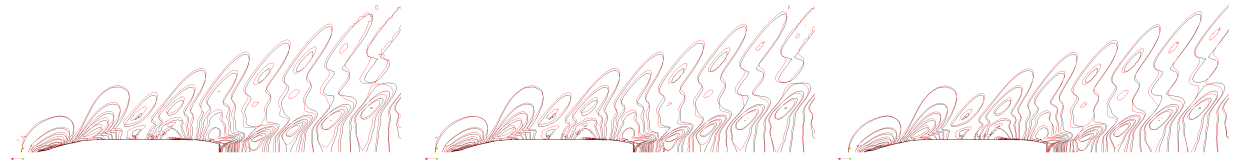

Fig. 7: Comparison of the wave patterns generated by the three selected hulls. Black one corresponds to the original KCS hull.

4 Conclusions

A surrogate model based sensitivity analysis of hull shape variations with respect to total resistance has been presented. A Kriging response surface has been used to predict the calm water resistance of the KCS hull subject to several geometric changes. The hull form variations have been achieved by means of a combined approach based on Subdivision Surface and Free Form Deformation. The effect of the size of the initial sampling on the performance of the surrogate model has been studied. Three sampling sizes

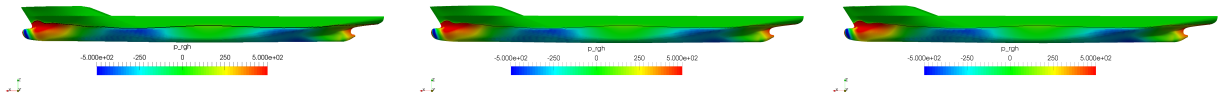

(a) (b) (c)

Fig. 8: Comparison of the dynamic pressures on the three selected hulls.

have been considered, namely 30, 60 and 120 designs.
Cross-validation on the three surrogate models shows that all the response surfaces have good prediction capabilities. However, the three optimum points on each surface have different combination of the design parameters. This highlight the fact that the size of the initial sampling affect the shape of the surrogate model and, in turn, the choice of the final best solution.
Further studies on ad-hoc infilling strategies will be performed since there is not a clear trend of the increase of the sampling size with respect to the accuracy of the solution.

References

Coppedé, A., Vernengo, G., and Villa, D. (2018). A combined approach based on subdivision surface and free form deformation for smart ship hull form design and variation. *Ships and Offshore Structures*.

Forrester, A., Keane, A., et al. (2008). *Engineering design via surrogate modelling: a practical guide*. John Wiley & Sons.

Gaggero, S., Villa, D., and Viviani, M. (2017). An extensive analysis of numerical ship self-propulsion prediction via a coupled bem/rans approach. *Applied Ocean Research*, 66:55–78.

Jasak, H., Jemcov, A., and Tukovic, Z. (2007). Openfoam: A c++ library for complex physics simulations. In *International workshop on coupled methods in numerical dynamics*, volume 1000, pages 1–20. IUC Dubrovnik, Croatia.

Lackenby, H. (1950). On the systematic geometrical variation of ship forms. *Trans INA*, 92:289–316.

Larsson, L., Stern, F., Visonneau, M., Hirata, N., Hino, T., and Kim, J. (2015). Tokyo 2015: A workshop on cfd in ship hydrodynamics. In *Proceedings of the Tokio 2015 Workshop - A Workshop on CFD in Ship Hydrodynamics*, volume 2, pages 1–1.

Peri, D. and Campana, E. F. (2003). Multidisciplinary design optimization of a naval surface combatant. *Journal of Ship Research*, 47(1):1–12.

Sederberg, T. W. and Parry, S. R. (1986). Free-form deformation of solid geometric models. *ACM SIGGRAPH computer graphics*, 20(4):151–160.

Stam, J. and Loop, C. (2003). Quad/triangle subdivision. In *Computer Graphics Forum*, volume 22, pages 79–85. Wiley Online Library.

Vernengo, G. and Brizzolara, S. (2017). Numerical investigation on the hydrodynamic performance of fast swaths with optimum canted struts arrangements. *Applied Ocean Research*, 63:76–89.

Vernengo, G., Brizzolara, S., Bruzzone, D., et al. (2015). Resistance and seakeeping optimization of a fast multihull passenger ferry. *International Journal of Offshore and Polar Engineering*, 25(01):26–34.

Villa, D., Gaggero, S., and Brizzolara, S. (2011). Simulation of ship in self propulsion with different CFD methods: From actuator disk to potential flow/RANS coupled solvers. In *RINA, Royal Institution of Naval Architects - Developments in Marine CFD, Papers*, pages 1–12.